Ab initio models for ZnS surfaces: Influence of cluster size on surface properties

Juha Muilu* and Tapani A. Pakkanen
Department of Chemistry, University of Joensuu, P.O. Box 111, Joensuu, SF-80101 Finland
(Received 16 June 1993)

The feasibility of the cluster method is studied using two-dimensional ZnS surface models. We used the translational symmetry of electron integrals in the Hartree-Fock valence method as it enables studies of large systems, containing several hundred atoms. The results show that the influences of boundaries and empty vacancies are limited only to a small area, and thus relatively small models can be used to simulate infinite systems. The properties are converging monotonically as the size of the model increases. However, in some cases small, size-dependent variations exist. Augmenting the minimal valence basis set with Zn 4*p* polarization functions decreases the influence of boundaries, and the charge distribution of surface becomes more uniform.

I. INTRODUCTION

In studying bulk and surface properties of crystals, cluster models have now been widely used. It is expected that finite models can be used to simulate infinite systems. Problems arising from the artificial termination of the model can be taken into account by special treatments like embedding and localization techniques[1–7] if necessary. On the other hand, ionic and covalent systems have fairly localized electronic structures, and thus the influences of the edges and other local effects are limited only to a small region of space. This makes it possible to use rather small models. Few studies have actually defined how large a model should be or how the electronic structure and the influence of local effects change when the size of the model varies. The aim of our work is to study the size effects and the influence of the edges of zinc sulfide surfaces as the size of the model increases. ZnS was chosen because its surface properties and phenomena are used in optoelectronic applications and because reference studies are available for comparison.[8–11]

Cluster techniques[12–14] are often based on *ab initio* molecular orbital (MO) methods, where MO's are constructed as linear combinations of atomic orbitals. The method proves advantageous because no empirical parameters are included and the accuracy level can be increased in a controlled fashion.[13] The method is based on the one used in molecular studies, and thus the same widely used programs can be utilized. Alternative approaches are the *ab initio* solid state techniques based on infinite models.[15,12] Although these methods give more accurate results for the bulk properties of crystals, local effects cannot be studied easily without repeating them within every symmetry unit. The common problem in both cases is the enormous number of many-particle interactions that need to be taken into account. In the Hartree-Fock theory, where interactions are self-consistently averaged, the number of two-particle components, the two-electron integrals, necessary for calculating and storing increases as N^4, where N is the number of orbitals. Recently, fast algorithms have been developed[16–18] for the integral calculations and the storage problems can be avoided by direct methods, where integrals are recalculated as needed.[19] Although the increase of two-electron integrals is not necessarily $O(N^4)$ in practice, they still pose a serious limit. In solid state techniques the translational symmetry of integrals over lattice vectors is traditionally used to reduce calculations. Nevertheless, similar treatments in cluster studies have not been used until recently.[20–22]

II. THEORY

In this work, the translational symmetry of core-valence and valence two-electron integrals have been used in Hartree-Fock (HF) –valence method. As described in our previous work,[22] it can be shown that only integrals with at least one basis function on two adjacent edges of slab need to be calculated. This has a marked effect, reducing the number of integrals necessary to calculate from $O(N^4)$ to $O(N^3)$. The number of translationally unique integrals (U) can be obtained from the equation

$$U(i,j,k,m) = Q(ijkm) - Q(ij[k-1]m) - Q(i[j-1]km) - Q([i-1]jkm) + Q(i[j-1][k-1]m) + Q([i-1]j[k-1]m) + Q([i-1][j-1]km) - Q([i-1][j-1][k-1]m), \quad (1)$$

where

$$Q(n) = \frac{1}{2}\left[\frac{n}{2}(n+1)\right]\left[s\frac{n}{2}(n+1)+1\right] \quad (2)$$

and m is the number of basis functions in the translational unit. Integers i,j, and k are the translations to the three directions in the model. For example, in the case of a five atoms wide and k atoms long slab of hydrogen

atoms with one basis function on each atom the number of integrals increases, $U(5,k,1,1) = -34 + 145.5k - 231k^2 + 184.5k^3$ when translational symmetry is used. Without translational symmetry the number of integrals increases as $Q(5\times k\times 1\times 1) = 1.25k + 9.375k^2 + 31.25k^3 + 78.125k^4$. A further reduction in the calculation can be obtained by estimating the magnitude of the integrals by the Schwartz inequality. The prescreening works very well for large models, where the relation of the integrals to be calculated vs basis functions approaches linear.[22]

The principles of the valence method have been described earlier.[23–25] The wave function is divided into valence and core orbitals according to the frozen core approximation. Valence orbitals are constructed as linear combinations of atomic orbitals and treated variationally in the fixed field of the atomic core. The core-valence orthogonality is preserved at two levels. One-center orthogonality is explicitly enforced by simple auxiliary functions representing the core orbitals. Two-center orthogonality to the neighboring nuclei is maintained by standard projection operator techniques. The core-valence interactions are described with density matrix approximations, where densities of core orbitals are expressed as Gaussian expansions. All approximations can be introduced stepwise and the uncertainly of each step can be estimated by error analysis. The Gaussian expansions and contracted basis functions are taken from previous work.[9] Valence basis functions for sulfur include $3s$ and $3p$ and $4s$ for zinc. D functions of zinc are kept in the core because they have been shown to have negligible influence on the valence electronic structure.[11] The influence of the basis functions is demonstrated by augmenting the Zn basis set by $4p$ functions. The role of the $4p$-polarization functions can be expected to be significant, since they allow the hybridization of the tetrahedrally coordinated zinc. The influence of the electron correlation has been tested with trial calculations on smaller models without translational symmetry. These studies were carried out with an effective core potential (ECP) double zeta basis set $(3d, 4s, 4p, 4d, 5s$, and $5p$ valence functions for zinc and $3s, 3p, 4s$, and $4p$ for sulfur) at MP2 level using the GAUSSIAN 92[26] program. The results for 1×1 and 2×2 Zn_3S_3-ring models gave energy lowering of 0.31% and 0.32% from the total energies, respectively. The qualitative structure of the charge distribution is not influenced by electron correlation.

III. SURFACE MODEL

In this work two-dimensional ZnS models are studied. Although the models differ from real, multilayer systems, it is expected that general, size-dependent trends can be seen. The slab models are computationally far less expensive than 3D models and can be studied more extensively, providing a basis for more demanding studies. Models consist of (111) cubic zinc-blende surfaces, which have an increasing number of ZnS rings, maintaining homogenous edges corresponding to low-index surface planes. Experimental bond lengths [R(Zn-S)=2.341 Å] and angles are used, and no reconstruction of the surface is considered. Distances between neighboring Zn (S) and Zn (S) atoms are 3.824 Å. An example of the surface model is in Fig. 1. The integral rejection threshold used is 10^{-6}. The influence of the threshold on the computational accuracy is demonstrated in Table I for the $Zn_{44}S_{44}$ sheet. The long and narrow sheet (2×15 ZnS rings) represent the worst case, where distances between function centers are

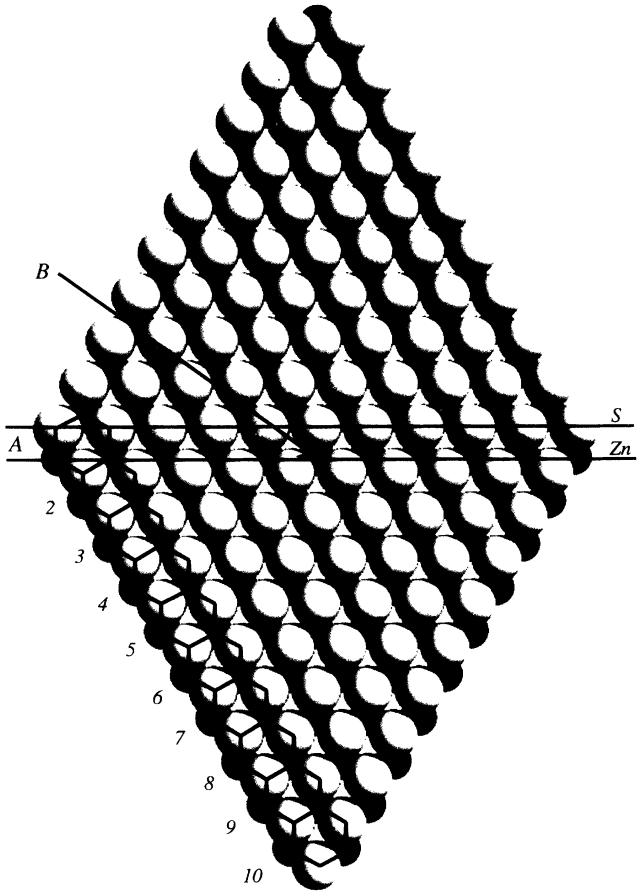

FIG. 1. 10×10 $Zn_{120}S_{120}$-surface model.

TABLE I. The influence of different integral rejection thresholds. Number of integrals needed, total energy per ZnS unit, HOMO energy, and maximum difference of charges are shown.

Threshold	Integrals needed	Total energy/ZnS	HOMO	Charge difference
10^{-5}	206835	-10.66947	-0.14057	-0.062
10^{-6}	372339	-10.67061	-0.14318	0.007
10^{-7}	580032	-10.67103	-0.14341	-0.003
10^{-8}	856565	-10.67106	-0.14331	-0.003
10^{-10}	1487474	-10.67106	-0.14331	0.000

large and most of the integrals vanish.

Models are labeled according to the number of Zn_3S_3 rings. For example, the $Zn_{120}S_{120}$ model in Fig. 1 is 10×10. If Zn $4p$-polarization functions are included, then character "p" is added after the label. The influence of local defects is studied by removing a Zn atom from the center of the sheet marked as B in Fig. 1. The charges in the graphs are taken from cross section A.

IV. RESULTS

A. Ideal surfaces

As the size of the model increases, the electronic properties should converge and the influence of the edges on the central site of the model should vanish. In principle, the convergence should be monotonical, if the symmetry and the topology remain the same.

The influence of cluster size on the charge distribution was studied using the Mulliken charges of atoms. Figure 2 gives the charges of the 7×7 and $7 \times 7p$ surfaces, including the differences of the charges from the mean value. The magnitude of the difference is indicated as size of a circle and the sign of the difference as a shade. Figure 2 shows that the influence of the boundaries decreases soon after moving away from the edges toward the center, and a relatively large area in the middle remain constant. The Zn $4p$-polarization functions decrease the magnitude of charges by about 50%. This effect may be partially due to the uncertainties in the Mulliken population analysis. The improvement in the basis set makes the charge distribution more uniform and the influence of the edges becomes smaller. Figure 3 gives the charges of atoms in cross section A of surface models containing one to one-hundred zinc sulfide rings. In all cases the charges change considerably from the edge atom to the next atom layer, and after this first large jump, they are converging rapidly while decreasing a little. The influence of size on the inner atoms is small and after the 4×4 model the charges remain almost constant. On the edges, there are minor and slightly converging variations between models. The variation is closely related to the oscillation of the charges along the boundaries, existing on all models larger than 3×3. This wavelike oscillation can be seen in Fig. 4, where the point charges of boundary atoms of models 1×15-5×15 are fitted into spline curves. Figure 4 shows that the oscillation exists on all except the smallest 1×15 and $1 \times 15p$ models. Otherwise, the size of the model has only a slight influence on the oscillation and only the "frequency" seems to change a little. In addition, the oscillation decreases when moving from the edge to the inside of the model as already seen on neighboring sulfur atoms. A better basis set also decreases the magnitude of the variation indicating the importance of the flexibility of basis set.

When the size of the model is increased, the proportion of the edge atoms atoms becomes smaller and the average energy of the ZnS unit should become more negative. This can be seen in Fig. 5. The energies converge monotonically but not as rapidly as the charge distribution. The influence of relative number of edge atoms is also seen at more negative energies of the $1 \times$ 1-10×10, $1 \times 1p$-$7 \times 7p$ models as compared to the linearly growing models. The zinc $4p$ basis lowers energies by about 0.1 a.u. The effect is more pronounced on larger models. The eigenvalue spectrum and the density of the states for models $1 \times$ 1-10×10 are shown in Fig. 6. As the size of the model increases lower s and upper sp bands become sharper, and the band structure becomes more evident. No sharp band gaps exists, because the orbitals on top of the bands are formed mainly from atomic orbitals centered on bare boundaries and are thus higher in energy. These boundary states are also responsible for

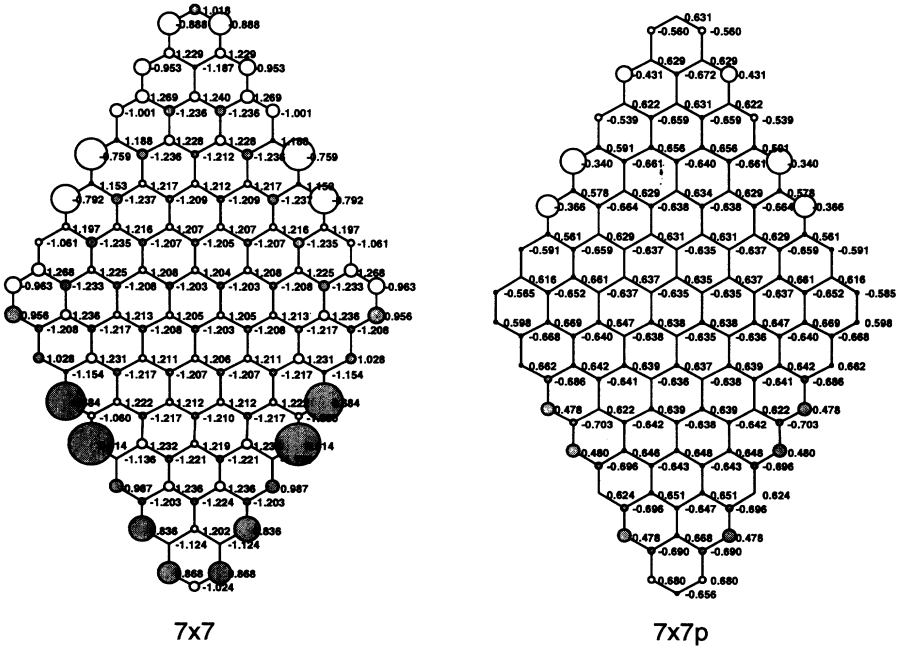

FIG. 2. Mulliken charges of 7×7 and $7 \times 7p$ surface models. Circles indicate the difference in charges from the mean value. Circles are shaded according to the sign of the difference

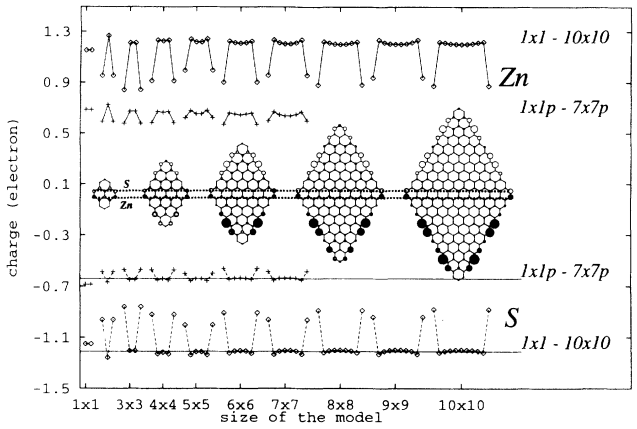

FIG. 3. Mulliken charges of Zn and S atoms in cross section A as the size of the model increases.

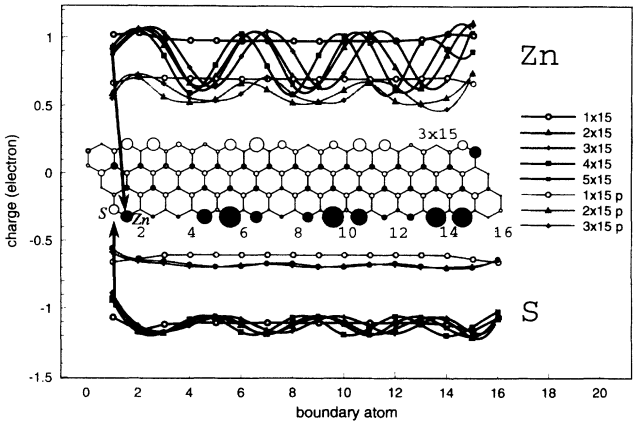

FIG. 4. Charges of boundary (Zn-edge) Zn and S atoms in models $1 \times 15\text{-}5 \times 15$ and $1 \times 15p\text{-}3 \times 15p$. Mulliken point charges are fitted to a spline curve.

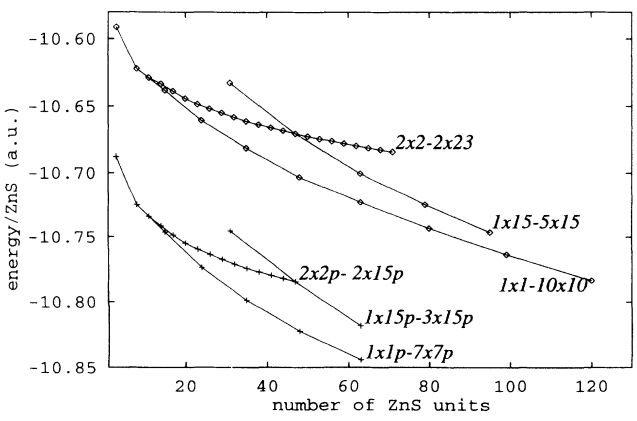

FIG. 5. Total energies of different models per ZnS unit as function of the size of the model.

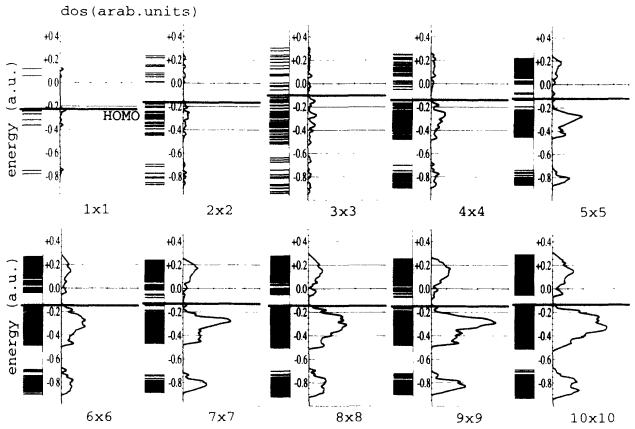

FIG. 6. Eigenvalue spectrum and density of states of $1\times1\text{-}10\times10$ ZnS models.

the low energies of unoccupied orbitals. Figure 6 also shows a small regular variation between models, which can be seen as a broadening of bands in cases having an even number of ZnS rings. Because highest occupied molecular-orbital (HOMO) energies are lower and lowest unoccupied molecular orbital (LUMO) higher in those cases, there are also fairly large fluctuations in the HOMO-LUMO gap, which changes within 0.04-0.1 a.u. (1.1 eV–2.7 eV). An augmented basis set decrease the HOMO and LUMO energies about 0.07 a.u., but it does not have much influence on the variation. The explanation to the variation might be the slightly different topology between the adjacent models. In real clusters[27–33] there are also size dependent effects, which arise from the node structure of the wave function confined within the potential walls of the finite system. This quantum size effect can lead to a stepwise variation in corresponding states as the size increases, because there is not necessarily an exact correspondence between the number of nodes and the dimensions of different models, and thus a small frequency shift is obtained. It is evident that the same kind of phenomenon is also seen in the current ZnS models. In Fig. 7 are the HOMO and LUMO energies

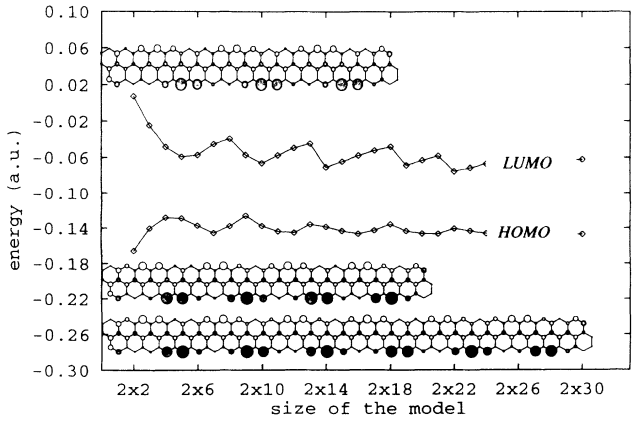

FIG. 7. HOMO and LUMO energies as functions of chain length.

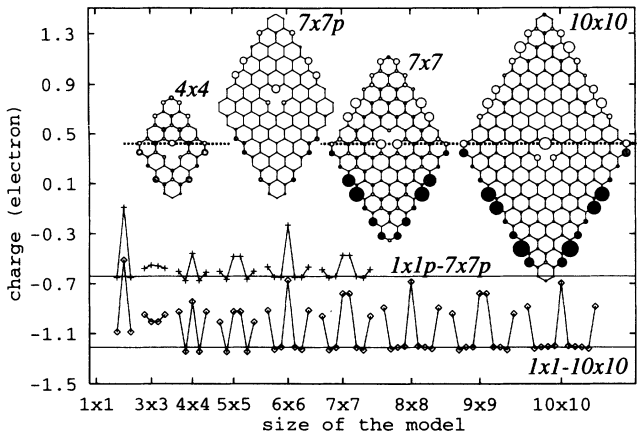

FIG. 8. Charges of sulfur atoms after Zn is removed. Charges of models $1 \times 1p$-$7 \times 7p$ and $1 \times$ 1-10 $\times$ 10 are taken from cross section *A*.

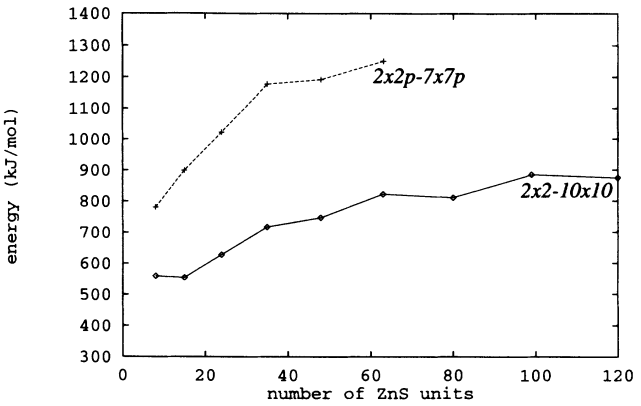

FIG. 9. Dissociation energies $E_d = E(\mathrm{Zn}_{x-1}\mathrm{S}_x) + E(\mathrm{Zn}) - E(\mathrm{Zn}_x\mathrm{S}_x)$ as the function of size of the model.

of models 2×2-2×30 along with the charge map of models with different chain lengths. Figure 7 shows that the variation in energies corresponds with the variation in charges at the edges. HOMO energies are lower in cases where the chain is cut, in places where the charges are close to the mean value. Again, the polarization basis set decrease the variation as it did for the charges.

B. Surface defects: The influence of vacancies

As already seen, the electronic structure is fairly local in ZnS systems, and thus the influence of vacancies like other local effects should converge rapidly as the model increases.

The effect of a vacancy was studied by removing the zinc atom from the center of the model. Figure 8 gives the charges of sulfur atoms in cross section *A* of Zn-deficient models $2 \times$ 2-10 $\times$ 10 and $2 \times 2p$-$7 \times 7p$. Figure 8 shows that the influence of the vacancy reaches, at most, to the nearest sulfur atoms only and has only a weak influence on the rest of the atoms. The influence is also becoming smaller as the model increases and remains almost constant after the model has reached the 4×4 size. The augmented basis set decreases the effects near vacancies in all cases, otherwise, the results are almost similar, differing the most in smaller models. The charges of the entire surfaces of 7×7 and $7 \times 7p$ are also in Fig. 8. Figure 8 shows that the influence of the Zn vacancy on the entire surface is quite small, especially on the augmented model.

Dissociation energies $E_d = E(\mathrm{Zn}_{x-1}\mathrm{S}_x) + E(\mathrm{Zn}) - E(\mathrm{Zn}_x\mathrm{S}_x)$ are in Fig. 9. Energies converge as the size of the model increases showing the increased difficulty of removing the zinc atom until the model has grown to a certain limit. The polarization basis set increases the stabilization energy about 250–400 kJ/mol, which seems to reach the final level in smaller models.

V. DISCUSSION

In this work the feasibility of the cluster method is demonstrated on zinc sulfide models. The influences of local effects like vacancies and boundaries are shown to be limited to a small region and thus quite reasonably sized models can be used to simulate infinite systems. However, properties do not necessarily converge smoothly, and in some cases, small, size-dependent variations exist. This effect, more pronounced by a poor basis set, may need attention in cases where models of different sizes or different sites are compared. The addition of the $4p$-polarization functions to the valence basis set of the Zn atom stabilizes the models. The charge distribution becomes more uniform, and the influences of local effects and boundaries decrease. The energies also seem to converge more rapidly to the final values.

* FAX: 358-73-1513344.

[1] J. L. Whitten, Phys. Rev. B **24**, 1810 (1981).
[2] P. V. Madhavan and J. L. Whitten, Surf. Sci. **112**, 38 (1981).
[3] P. Cremaschi and J. L. Whitten, Surf. Sci. **112**, 343 (1981).
[4] B. N. Dev, K. C. Mishra, W. M. Gibson, and T. P. Das, Phys. Rev. B **29**, 1101 (1984).
[5] C. Pisani, D. R. R. Nada, and L. N. Kantorovich, J. Chem. Phys. **92**, 7448 (1990).
[6] Y. Fukunishi and N. Nakatsuji, J. Chem. Phys. **97**, 6535 (1992).
[7] J. D. Head and S. J. Silva, Int. J. Quantum Chem. Symp. **26**, 229 (1992).
[8] T. A. Pakkanen, V. Nevalainen, M. Lindblad, and P. Makkonen, Surf. Sci. **188**, 456 (1987).
[9] M. Lindblad and T. A. Pakkanen, J. Comput. Chem. **9**, 581 (1988).
[10] K. Tóth, T. A. Pakkanen, P. Hirva, and J. Muilu, Surf. Sci.

277, 395 (1992).
[11] K. Tóth and T. A. Pakkanen, J. Comput. Chem. **14**, 667 (1993).
[12] J. Sauer, Chem. Rev. **89**, 199 (1989).
[13] P. S. Bagus, in *Elemental and Molecular Clusters*, edited by G. Benedek, T. P. Martin, and G. Pacchioni, Springer Series in Materials Science Vol. 6 (Springer-Verlag, Berlin, 1987), p. 286.
[14] P. E. M. Siegbahn, L. G. M. Pettersson, and U. Wahlgren, J. Chem. Phys. **94**, 4024 (1991).
[15] C. Pisani, R. Dovesi, and C. Roetti, *Hartree-Fock Ab Initio Treatment of Crystalline Systems*, Lecture Notes in Chemistry Vol. 48 (Springer-Verlag, Berlin, 1988).
[16] S. Obara and A. Saika, J. Chem. Phys. **84**, 3963 (1986).
[17] M. Head-Gordon and J. A. Pople, J. Chem. Phys. **89**, 5777 (1988).
[18] R. Lindh, U. Ryu, and B. Liu, J. Chem. Phys. **91**, 5889 (1991).
[19] J. Amlöf, K. Faegri, and K. Korsell, J. Comput. Chem. **3**, 385 (1981).
[20] T. A. Pakkanen, Ph.D. thesis, State University of New York at Stony Brook, 1977.
[21] J. D. Head and I. P. Dillon, Theor. Chim. Acta **78**, 231 (1991).
[22] T. A. Pakkanen and J. Muilu, Theor. Chim. Acta **86**, 285 (1993).
[23] T. A. Pakkanen and J. L. Whitten, J. Chem. Phys. **69**, 2168 (1978).
[24] J. L. Whitten and T. A. Pakkanen, Phys. Rev. B **21**, 4357 (1980).
[25] T. A. Pakkanen, M. Lindblad, and R. S. Laitinen, Int. J. Quantum Chem. **29**, 1789 (1986).
[26] M. J. Frisch *et al.*, GAUSSIAN 92, Revision B, Gaussian, Inc. Pittsburgh, PA, 1992.
[27] R. C. Jaklevic and L. J., Phys. Rev. B **12**, 4146 (1975).
[28] R. Rossetti, J. L. Ellison, J. M. Gibson, and L. E. Brus, J. Chem. Phys. **80**, 4464 (1984).
[29] R. Rossetti, R. Hull, J. M. Gibson, and L. E. Brus, J. Chem. Phys. **82**, 552 (1985).
[30] E. E. Mola and J. L. Vicente, J. Chem. Phys. **84**, 2876 (1986).
[31] Y. Wang and N. Herron, J. Phys. Chem. **95**, 525 (1991).
[32] J. Jortner, Z. Phys. D **24**, 247 (1992).
[33] J. C. Boettger and S. B. Trickey, Phys. Rev. B **45**, 1363 (1992).

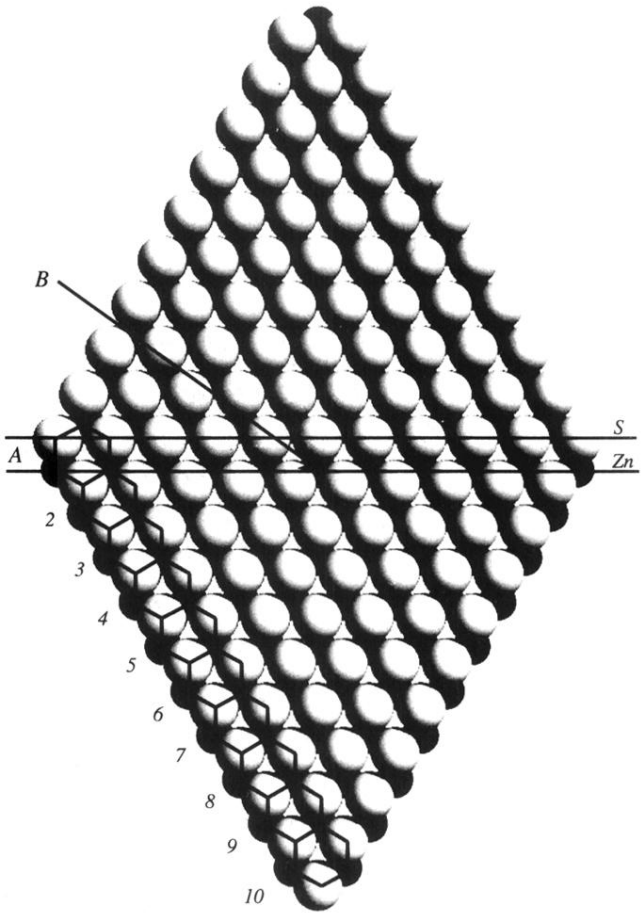

FIG. 1. 10×10 $Zn_{120}S_{120}$-surface model.

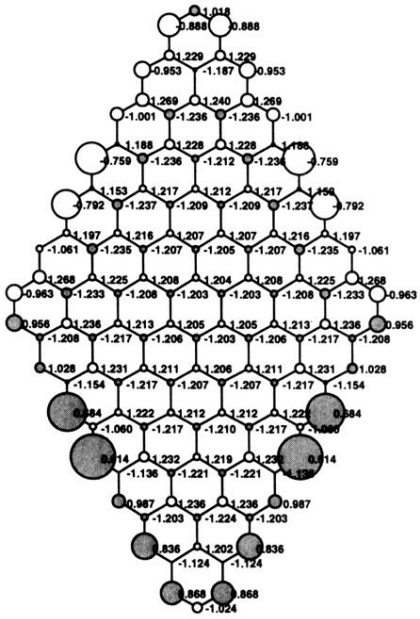

7x7

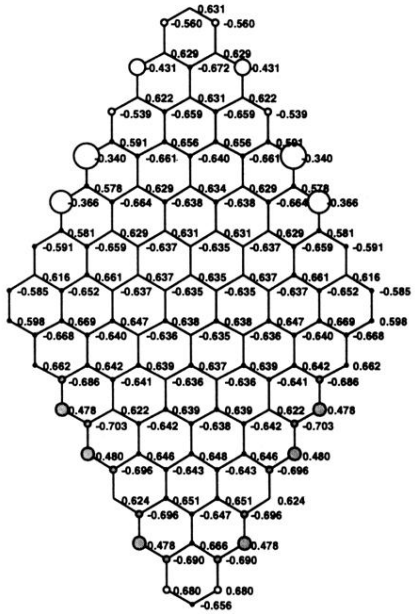

7x7p

FIG. 2. Mulliken charges of 7×7 and $7 \times 7p$ surface models. Circles indicate the difference in charges from the mean value. Circles are shaded according to the sign of the difference

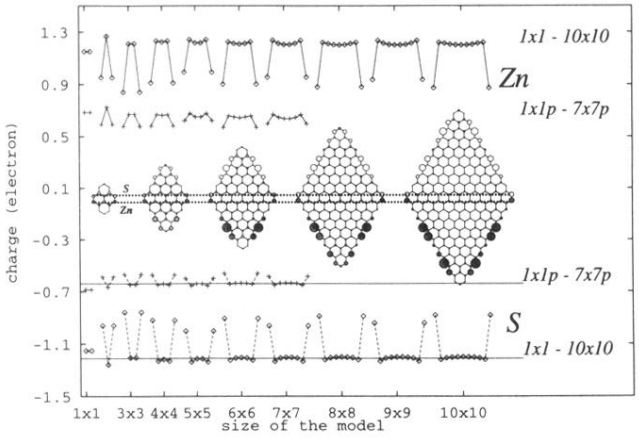

FIG. 3. Mulliken charges of Zn and S atoms in cross section *A* as the size of the model increases.

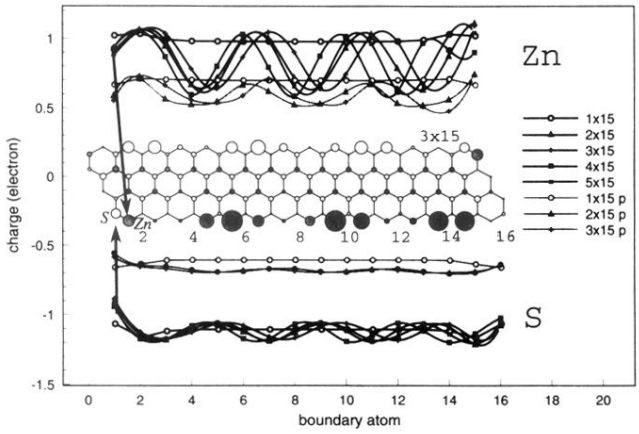

FIG. 4. Charges of boundary (Zn-edge) Zn and S atoms in models 1×15-5×15 and $1 \times 15p$-$3 \times 15p$. Mulliken point charges are fitted to a spline curve.

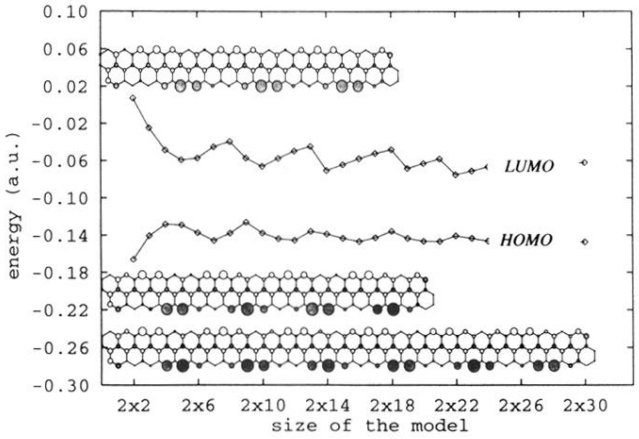

FIG. 7. HOMO and LUMO energies as functions of chain length.

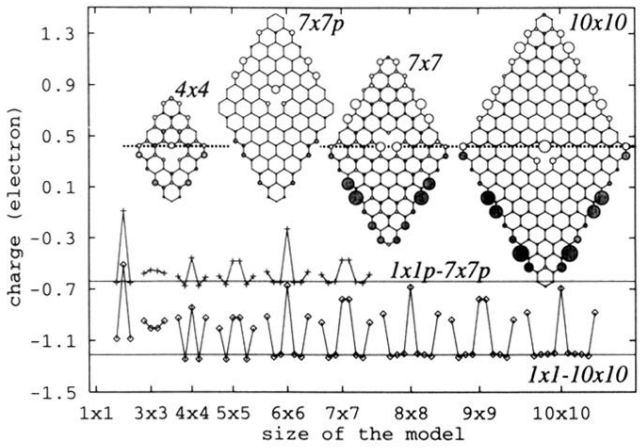

FIG. 8. Charges of sulfur atoms after Zn is removed. Charges of models $1 \times 1p$-$7 \times 7p$ and $1 \times$ 1-10×10 are taken from cross section *A*.